

Effect of rare-gas adsorption on the spin-orbit split bands of a surface alloy: Xe on Ag(111)-($\sqrt{3} \times \sqrt{3}$)R30°-Bi

L. Moreschini,¹ A. Bendounan,^{2,3} C. R. Ast,⁴ F. Reinert,² M. Falub,¹ and M. Grioni¹¹*Institut de Physique des Nanostructures, Ecole Polytechnique Fédérale de Lausanne (EPFL), CH-1015 Lausanne, Switzerland*²*Experimentelle Physik II, Universität Würzburg Am Hubland, D-97074 Würzburg, Germany*³*Laboratory for Neutron Scattering (LNS), ETH Zurich and Paul Scherrer Institut (PSI), CH-5232 Villigen PSI, Switzerland*⁴*Max-Planck-Institut für Festkörperforschung, D-70569 Stuttgart, Germany*

(Received 8 January 2008; published 5 March 2008)

We have investigated by angle-resolved photoemission spectroscopy changes induced by Xe adsorption on the spin-orbit-split bands of the epitaxial Ag(111) ($\sqrt{3} \times \sqrt{3}$)R30°-Bi surface alloy. We observe an extensive backfolding of the alloy band structure due to the formation of a 9×9 commensurate or quasicommensurate Xe overlayer and the opening of a small hybridization gap at the intersection of two sets of bands of (primarily) Bi sp_z and p_{xy} characters. The large spin-orbit splitting of the substrate bands is essentially unaffected by the Xe overlayer, in sharp contrast to the enhancement reported for the clean Au(111) surface. This points to different mechanisms at the origin of the splitting in the clean surfaces and in the surface alloy.

DOI: 10.1103/PhysRevB.77.115407

PACS number(s): 68.43.-h, 68.47.De, 71.70.Ej, 79.60.Dp

I. INTRODUCTION

Rare-gas overlayers on metal surfaces are a subject of interest for their structural properties^{1–5} and especially for the modifications induced on the electronic structure of the substrate.^{6–10} The electronic properties of the interface ultimately depend on the delicate interplay between the long-range attractive van der Waals forces and the short-range Pauli repulsion, which produce a characteristic adsorption potential for each substrate-adsorbate system. For adsorption on metal surfaces with occupied surface states, e.g., the Shockley states at the (111) surfaces of noble metals, the dominant term is the electrostatic interaction between the substrate and the polarized electronic shell of the adsorbate,¹⁰ but the repulsion due to wave-function overlap is still responsible for the reduction of the binding energy (E_B).^{9,11}

The spin degeneracy of these surface states is lifted due to the lack of structural inversion symmetry and to the spin-orbit (SO) interaction, and their two-dimensional parabolic dispersion is modified.^{12,13} For any direction within the surface, angle-resolved photoemission spectroscopy (ARPES) shows two split maxima at symmetric ($\pm k_0$) locations around the center of the surface Brillouin zone (BZ). The free-electron model developed by Rashba (RB) for semiconductors¹⁴ or a more detailed tight-binding model¹⁵ provides a qualitative interpretation of the ARPES data. In both models, the gradient of the electric potential plays a crucial role, but while the former only takes into account an effective electric field, the latter distinguishes between an atomic SO interaction and a contribution from the surface potential gradient. A quantitative description has been achieved by first-principles relativistic calculations.¹⁶ ARPES experiments have also shown that the SO splitting of the Au(111) Shockley state increases with the adsorption of three noble gases (Ar, Kr, Xe).¹¹ The action of the adsorbate is twofold: it changes the surface potential and pushes the wave function of the surface state closer to the nucleus of the substrate atoms, where the potential is steepest.¹⁷

Recently, it was shown by ARPES and scanning tunneling microscopy that SO splittings up to 1 order of magnitude larger than for Au(111) can be achieved in substitutional XAg_2 alloys formed by large- Z metals ($X=Pb, Bi$) at the Ag(111) surface.^{18–20} In these alloys, bismuth (lead) atoms replace one out of three silver atoms in the topmost layer, yielding an ordered ($\sqrt{3} \times \sqrt{3}$)R30° structure.²¹ The positive effective mass ($m^* > 0$) Shockley state of the substrate is replaced by new ($m^* < 0$) bands, which result from the hybridization between the Bi p and the Ag sp states.

In the present paper, we explore by ARPES the effect of rare-gas adsorption on the Ag(111) ($\sqrt{3} \times \sqrt{3}$)R30°-Bi surface alloy, namely, the possibility of further increasing the SO splitting of the hybrid band states. We choose Xe because it yields the largest SO enhancement on the clean Au(111) surface¹⁰ and because its relatively high adsorption temperature ($T \approx 60$ K) favors the formation of a well-ordered overlayer with a low density of structural defects and impurities. We find that the dispersion of the alloy states, as measured by ARPES, is modified in two ways: (i) the bands are extensively backfolded and follow the overlayer-induced superlattice periodicity; (ii) small energy gaps appear at the avoided crossing of bands of (mainly) Bi sp_z and Bi p_{xy} characters. We also find that the Xe adsorption does not modify the SO splitting, in sharp contrast with the related case of the clean Au(111) surface.

II. EXPERIMENTAL DETAILS

We prepared clean ordered Ag(111) surfaces by repeated cycles of Ar⁺ sputtering and annealing at 800 K. The surface alloy was obtained by evaporation of 1/3 of a monolayer of Bi on the hot substrate ($T > 400$ K) to obtain an ordered ($\sqrt{3} \times \sqrt{3}$)R30° structure, as confirmed by low energy electron diffraction (LEED) [Fig. 1(a)]. The LEED pattern shows faint extra spots, which we attribute to a slight Bi excess leading to the formation of small Bi monolayer patches.²² The surface was then cooled down to 60 K and exposed for

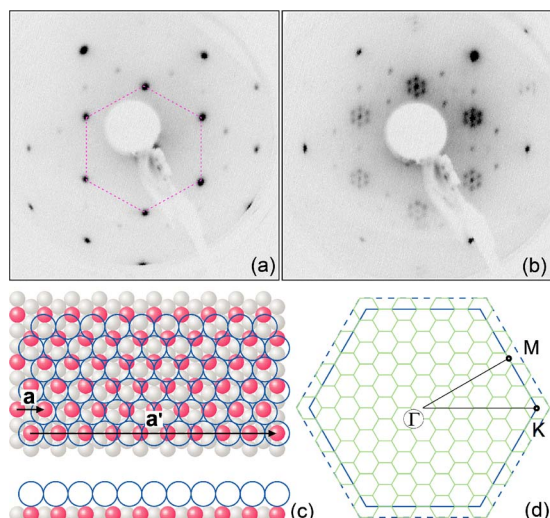


FIG. 1. (Color online) LEED pattern of the Ag(111) ($\sqrt{3} \times \sqrt{3}$) $R30^\circ$ -Bi surface alloy (a) before and (b) after Xe adsorption. The reciprocal space hexagonal unit cell of the alloy is traced in (a) for clarity. (c) Schematics (top and side views) of a commensurate 9×9 Xe-Ag(111) ($\sqrt{3} \times \sqrt{3}$) $R30^\circ$ -Bi structure, showing the hexagonal unit vectors \mathbf{a} of the substrate and $\mathbf{a}' = 9\mathbf{a}$ of the superlattice. Ag, gray filled circles; Bi, red (dark gray) filled circles; Xe, empty circles. The relaxations of the BiAg₂ layer and of the overlayer are neglected. (d) The surface BZs of the substrate are shown in blue (black) and that of the superlattice in green (gray). The large dashed hexagon is the BZ of the isolated Xe overlayer.

1 min to a Xe partial pressure of 3×10^{-8} mbar. These parameters were chosen in order to prevent the formation of multilayer coverages, which occurs at lower substrate temperatures and/or higher gas pressures. The formation of an ordered Xe monolayer is revealed by the appearance of six additional spots around each spot of the ($\sqrt{3} \times \sqrt{3}$) $R30^\circ$ LEED pattern [Fig. 1(b)]. ARPES measurements were performed with consistent results in Würzburg and Lausanne. Results are presented here from the former, more extensive data set. We used a high-brightness monochromatized helium lamp and a high-resolution hemispherical analyzer (Gamma-data R4000). The large acceptance angle ($\pm 15^\circ$) of the spectrometer allowed a large part of the surface BZ along one high-symmetry direction to be covered in a single measurement. The energy resolution was 3 meV, while the angular resolution was 0.3° . The Xe/Bi/Ag(111) surface structure was checked by LEED at the end of each ARPES experiment.

III. RESULTS AND DISCUSSION

The adsorption of Xe on (111) metal surfaces results in the formation of a close-packed hexagonal overlayer with a ($\sqrt{3} \times \sqrt{3}$) $R30^\circ$ superstructure whenever the quantity $d^* = \sqrt{3} \times \text{NN}$ (NN=substrate nearest-neighbor distance) is close to $d_{\text{Xe-Xe}} = 4.4$ Å, the Xe-Xe separation in solid Xe. This is, e.g., the case for copper (4.41 Å), palladium (4.76 Å), and platinum (4.8 Å). For clean Ag(111), $d^* = 5$ Å, and Xe rather forms a nonrotated and slightly ex-

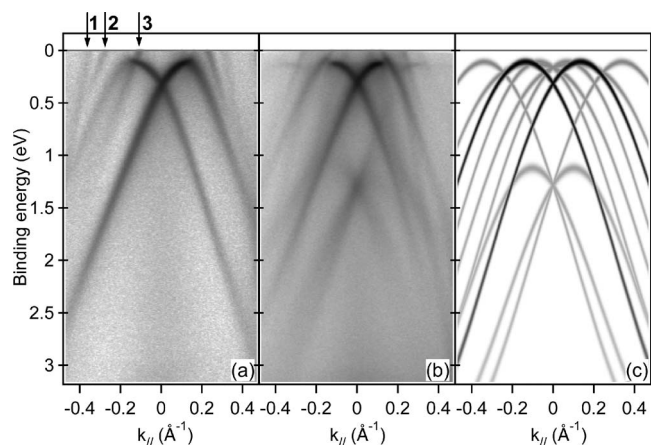


FIG. 2. The measured band structure along the $\bar{M}\bar{\Gamma}\bar{M}$ high-symmetry direction (a) before and (b) after Xe adsorption. $k_{\parallel} = 0$ corresponds to the $\bar{\Gamma}$ point. The intensity is plotted on a logarithmic scale to enhance the weaker backfolded features. (c) shows a simple calculation of the expected band dispersion for an umklapp of the two high intensity bands in panel (a) according to a 9×9 superperiodicity. Only the six BZs surrounding the central one are taken into account.

panded ($d_{\text{Xe}} = 4.5$ Å) incommensurate overlayer.^{1,2,23} By contrast, the LEED pattern of Fig. 1(b) shows that the Xe overlayer is aligned with the hexagonal lattice of the alloy, i.e., it is rotated by 30° with respect to the original Ag lattice, despite the similarity of the in-plane distances of the two substrates. This difference may be due to the larger corrugation of the alloy.^{23,24} Inspection of the LEED pattern suggests that the superlattice is commensurate, or quasicommensurate, with a periodicity equal to 9×9 that of the alloy. Assuming that Xe forms as usual a close-packed monolayer, this periodicity corresponds to an in-plane Xe separation equal to $9/10$ the Bi-Bi distance, or 4.49 Å, i.e., to a slightly expanded overlayer. The corresponding ideal structure is illustrated in Fig. 1(c). A quantitative structural investigation is needed to determine the buckling, which is present in the substrate, as shown, e.g., by surface x-ray diffraction for the PbAg₂ alloy,²⁵ and most likely also in the overlayer. Figure 1(d) illustrates the hexagonal BZ of the alloy and that of the 9×9 superlattice in the repeated zone scheme. The dashed hexagon represents the BZ of the isolated Xe overlayer.

The ARPES results are shown in Fig. 2 for the Bi/Ag(111) alloy (a) and for the Xe-covered surface (b) as photoemission intensity maps. Both panels show the band structure along the high-symmetry $\bar{M}\bar{\Gamma}\bar{M}$ direction [Fig. 1(d)]. The data for the clean substrate are in excellent agreement with those published in Ref. 18, but the broader angular window of the present data provides a better overview of all the relevant spectral features. The dominant features are two symmetric spin-orbit split bands, with maxima at wave vectors $k_0 = \pm 0.13$ Å⁻¹ and 0.13 eV binding energy, and an effective mass $m^* = -0.35m_e$. These bands result from the hybridization of Bi *p* and Ag *sp* states and mainly have *sp_z* (normal to the surface) character. A second set of symmetric spin-orbit split bands, of mainly *p_{xy}* (in-plane) character, is shifted upward in energy relative to the main *sp_z* bands, and

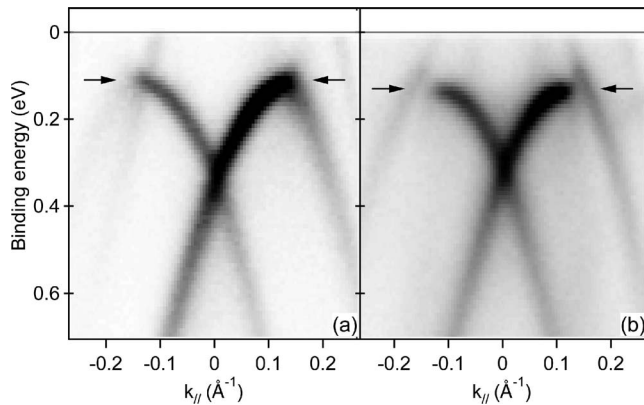


FIG. 3. ARPES data near the center of the surface BZ (a) before and (b) after Xe adsorption.

their maxima lie above the Fermi level. Their Fermi level crossings are identified, for $k_{\parallel} < 0$, by markers “2” and “3” in Fig. 2(a). The spectral weight distribution among these bands is strongly uneven due to ARPES transition matrix elements that depend on the polarization of the UV beam and on the experimental geometry.²⁶ The figure also shows, at larger wave vectors, a steeper band crossing the Fermi level in correspondence of marker “1.” It is the replica of the bulk Ag s conduction band, backfolded by the $(\sqrt{3} \times \sqrt{3})R30^\circ$ alloy superlattice.

The dispersion of the spin-orbit split bands is largely unaffected by the Xe overlayer [Fig. 2(b)]. In particular, their momentum separation remains unchanged. The most obvious change after the Xe adsorption is the appearance of several new weak features. They are offset on both sides of the $\bar{\Gamma}$ point, and their dispersion mimics the dispersion of the main bands. In particular, a well-defined crossing point between two (or more) bands appears at $\bar{\Gamma}$ at ≈ 1.3 eV. All features become fainter and less defined toward the edges of the image, where they enter the continuum of the projected Ag bulk states. The new bands are due to the backfolding of the alloy bands induced by scattering of the photoelectrons by the Xe overlayer. The measured data are qualitatively reproduced in Fig. 3(c) by an isotropic band matching the sp_z band dispersion, plus its 9×9 umklapps (for clarity, only the BZs of the 9×9 structure surrounding the first BZ were taken into account). The remaining differences are due to the backfolded p_{xy} bands, which are not considered in this simple model. Moreover, the main bands are not really isotropic but “feel” the lattice potential. Extended ARPES data and first-principles band structure calculations indeed show that away from $\bar{\Gamma}$, the constant-energy contours continuously evolve from a free-electron-like circle to a hexagon and finally to a hexagonal “flowerlike” shape for larger k_{\parallel} values.¹⁸

A closer inspection of the data near the crossing point between the sp_z and p_{xy} bands reveals a more subtle and interesting change. It is illustrated in Fig. 3, where the region close to the Fermi level around the $\bar{\Gamma}$ point is shown in greater detail. Despite the uneven intensity distribution, it is apparent from the map of Fig. 3(a) that the bands cross near the maxima of the sp_z bands (in correspondence of the arrows), indicative of a very small hybridization. The situation

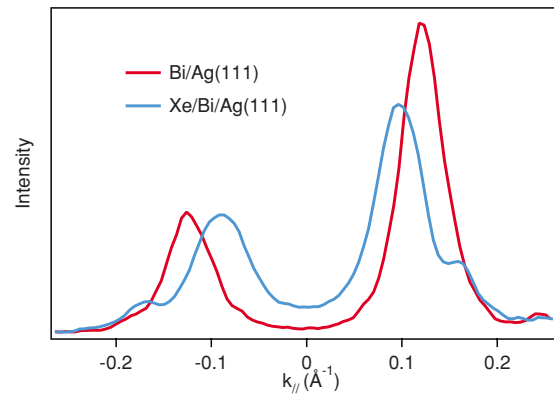


FIG. 4. (Color online) MDCs for the clean (red–dark gray) and for the Xe-covered alloy (blue–light gray) measured in correspondence of the horizontal arrows of Figs. 3(a) and 3(b), i.e., at $E_B = 0.11$ eV and $E_B = 0.13$ eV, respectively.

for the Xe-covered surface, illustrated in Fig. 3(b), is different. Here, we observe an avoided crossing and the opening of a small but clearly visible energy gap, marked by the arrows. Spectral weight is transferred from the lower to the upper band, whose dispersion also deviates from the straight line of Fig. 3(a). These changes are further confirmed by the momentum distribution curves (MDCs) of Fig. 4. The MDCs were measured at the crossing point of the sp_z and p_{xy} bands ($E_B = 0.11$ eV) for the pure alloy and at $E_B = 0.13$ eV for the Xe-covered surface. The well-defined peaks observed at $\pm 0.13 \text{ \AA}^{-1}$ for the clean alloy are clearly split after the formation of the rare-gas overlayer, revealing the hybridization between the two bands. Two independent first-principles calculations for the Bi/Ag(111) surface alloy find a non-negligible interaction between the sp_z and p_{xy} bands.^{18,27} They also find, however, that the hybridization strength is rather sensitive to the actual relaxation of the topmost layer, i.e., to the distance between the protruding Bi atom and the Ag surface. The observation of a stronger hybridization is consistent with a reduction of the Bi-Ag distance induced by the Xe overlayer.

The data of Figs. 2 and 3 suggest that the adsorption of rare-gas overlayers is probably not a viable strategy to further enhance the large energy and momentum splitting obtained in substitutional surface alloys. This contrasts with the larger splittings measured upon rare-gas adsorption on the clean Au(111) surface and also upon the reactive chemisorption of H and Li on metal surfaces.^{28,29} Notice that the orbital character of the split bands, mostly p -like, is similar to that of the Au Shockley states, and one might expect a similar influence of the overlayer. Nonetheless, this negative result may contribute to a better understanding of the mechanism behind the “giant” effect measured in the alloy, considerably larger not only than in Au(111) but also with respect to that found in the (111) face of large- Z metals.^{30,31} Neither the standard RB model, based on the surface potential gradient, nor the simple inclusion of the ionic potential seems able to explain this experimental result. Likewise, a virtual crystal approach,³² which interpolates between the properties of the two constituents, is obviously incompatible with the fact that

the momentum splitting in the Bi/Ag(111) alloy is larger than that in pure Bi (by a factor of 2.5) or in pure Ag (by a factor of 30). It has been proposed that the anomalously large size of the SO splitting in the surface alloys is the consequence of a large in-plane potential gradient, associated with the sixfold coordination of Bi by the Ag atoms.^{18,27} This possibility, which is usually not considered within the implementations of the RB model, is supported by two clear experimental observations: (i) the already mentioned anisotropic shape of the constant-energy contours and (ii) the recent observation in spin-resolved ARPES experiments of a sizable out-of-plane component of the spin polarization.³³ The latter scenario is incompatible with a purely out-of-plane potential gradient and requires an in-plane component. Interestingly, both these results are correctly predicted by first-principles calculations.^{18,27} This hypothesis is further supported by a recent free-electron model calculation, where the strength of the in-plane gradient could be varied as a parameter.³⁴

The adsorption of a rare gas on a metallic surface is expected to affect primarily the out-of-plane component of the surface potential.¹³ Therefore, the null effect on the Bi/Ag(111) alloy, where the SO splitting is mainly determined by the in-plane gradient, is apparently understood. However, the Xe layer has also an indirect effect on the SO splitting, through the hybridization of the sp_z and p_{xy} bands, because the in-plane gradient acts more strongly on the xy component of the wave function. A stronger hybridization mixes a larger xy character into the sp_z band, and a larger splitting would be expected. We have observed the signature of a larger hybridization but no increase of the SO splitting. We speculate that an effect of opposite sign may be at work,

namely, a reduction of the in-plane gradient as a consequence of the variation of the relaxation of the Bi layer. Unfortunately, it is not easy to predict how the gradient depends on the structural parameters of the interface. Detailed calculations are clearly required to elucidate this point.

IV. CONCLUSIONS

We have investigated the effect of the adsorption of a Xe layer on the electronic structure of the substitutional Bi/Ag(111) surface alloy. Our ARPES data indicate that the rare gas affects the relaxation of the topmost layer and enhances the interaction between the sp_z and p_{xy} bands of the alloy. The giant SO splitting of these bands is not modified by the overlayer, in contrast to the case of Ar, Kr, and Xe adsorption on the Au(111) surface. This different behavior is compatible with the hypothesis of different predominant parameters determining the SO splitting: an out-of-plane surface gradient in the case of the clean surface and an in-plane gradient in the surface alloy. Since the actual SO splitting depends on the precise values of the structural parameters, realistic calculations are required to achieve a quantitative description of the complex interface.

ACKNOWLEDGMENTS

We gratefully acknowledge J. Henk for many illuminating discussions. The work in Würzburg was possible thanks to the financial support by the Deutsche Forschungsgemeinschaft (Re1469/4-3). The work in Lausanne has been supported by the Swiss National Science Foundation and NCCR MaNEP.

-
- ¹M. Chesters, M. Hussain, and J. Pritchard, *Surf. Sci.* **35**, 161 (1973).
- ²J. Unguris, L. Bruch, and M. Webb, *Surf. Sci.* **114**, 219 (1982).
- ³J. M. Gottlieb, *Phys. Rev. B* **42**, 5377 (1990).
- ⁴R. Diehl, T. Seyller, M. Caragiu, G. Leatherman, N. Ferralis, K. Pussy, P. Kaukasoina, and M. Lindroos, *J. Phys.: Condens. Matter* **16**, S2839 (2004).
- ⁵N. Ferralis, H. Li, K. Hanna, J. Stevens, H. Shin, F. Pan, and R. Diehl, *J. Phys.: Condens. Matter* **19**, 056011 (2007).
- ⁶R. Behm, C. Brundle, and K. Wandelt, *J. Chem. Phys.* **85**, 1061 (1986).
- ⁷E. Bertel and N. Memmel, *Appl. Phys. A: Mater. Sci. Process.* **63**, 523 (1996).
- ⁸R. Paniago, R. Matzdorf, G. Meister, and A. Goldmann, *Surf. Sci.* **325**, 336 (1995).
- ⁹M. Wolf, E. Knoesel, and T. Hertel, *Phys. Rev. B* **54**, R5295 (1996).
- ¹⁰C. Hückstädt, S. Schmidt, S. Hüfner, F. Forster, F. Reinert, and M. Springborg, *Phys. Rev. B* **73**, 075409 (2006).
- ¹¹F. Forster, S. Hüfner, and F. Reinert, *J. Phys. Chem. B* **108**, 14692 (2004).
- ¹²S. Lashell, B. A. McDougall, and E. Jensen, *Phys. Rev. Lett.* **77**, 3419 (1996).
- ¹³F. Reinert, G. Nicolay, S. Schmidt, D. Ehm, and S. Hüfner, *Phys. Rev. B* **63**, 115415 (2001).
- ¹⁴Y. B. E. Rashba, *JETP Lett.* **39**, 78 (1984).
- ¹⁵L. Petersen and P. Hedegård, *Surf. Sci.* **459**, 49 (2000).
- ¹⁶J. Henk, A. Ernst, and P. Bruno, *Phys. Rev. B* **68**, 165416 (2003).
- ¹⁷F. Forster, A. Bendounan, F. Reinert, V. G. Grigoryan, and M. Springborg, *Surf. Sci.* **601**, 5595 (2007).
- ¹⁸C. R. Ast, J. Henk, A. Ernst, L. Moreschini, M. C. Falub, D. Pacilé, P. Bruno, K. Kern, and M. Grioni, *Phys. Rev. Lett.* **98**, 186807 (2007).
- ¹⁹C. R. Ast, G. Wittich, P. Wahl, R. Vogelgesang, D. Pacilé, M. C. Falub, L. Moreschini, M. Papagno, M. Grioni, and K. Kern, *Phys. Rev. B* **75**, 201401(R) (2007).
- ²⁰D. Pacilé, C. R. Ast, M. Papagno, C. Da Silva, L. Moreschini, M. Falub, A. P. Seitsonen, and M. Grioni, *Phys. Rev. B* **73**, 245429 (2006).
- ²¹J. Dalmas, H. Oughaddou, C. Leandri, J.-M. Gay, G. Le Gay, G. Treglia, B. Aufray, O. Bunk, and R. L. Johnson, *Phys. Rev. B* **72**, 155424 (2005).
- ²²The electronic structure of a full monolayer of Bi on Ag(111), which we have separately studied, is clearly distinct from that of the alloy. Its contribution to the ARPES spectra (Figs. 2 and 3) is weak and cannot be distinguished from the background.

- ²³J. Unguris, L. Bruch, E. Moog, and M. Webb, *Surf. Sci.* **87**, 415 (1979).
- ²⁴A. D. Novaco and J. P. McTague, *Phys. Rev. Lett.* **38**, 1286 (1977).
- ²⁵J. Dalmas, H. Oughaddou, G. Le Lay, B. Aufray, G. Tréglia, C. Girardeaux, J. Bernardini, J. Fujii, and G. Panaccione, *Surf. Sci.* **600**, 1227 (2006).
- ²⁶J. Henk, M. Hoesch, J. Osterwalder, A. Ernst, and P. Bruno, *J. Phys.: Condens. Matter* **16**, 7581 (2004).
- ²⁷G. Bihlmayer, S. Blügel, and E. V. Chulkov, *Phys. Rev. B* **75**, 195414 (2007).
- ²⁸E. Rotenberg, J. W. Chung, and S. D. Kevan, *Phys. Rev. Lett.* **82**, 4066 (1999).
- ²⁹M. Hochstrasser, J. G. Tobin, E. Rotenberg, and S. D. Kevan, *Phys. Rev. Lett.* **89**, 216802 (2002).
- ³⁰Y. M. Koroteev, G. Bihlmayer, J. E. Gayone, E. V. Chulkov, S. Blügel, P. M. Echenique, and P. Hofmann, *Phys. Rev. Lett.* **93**, 046403 (2004).
- ³¹K. Sugawara, T. Sato, S. Souma, T. Takahashi, M. Arai, and T. Sasaki, *Phys. Rev. Lett.* **96**, 046411 (2006).
- ³²H. Cercellier, C. Didiot, Y. Fagot-Revurat, B. Kierren, L. Moreau, D. Malterre, and F. Reinert, *Phys. Rev. B* **73**, 195413 (2006).
- ³³F. Meier, H. Dil, J. Lobo-Checa, L. Patthey, and J. Osterwalder, arXiv:0802.1125 (unpublished).
- ³⁴J. Prempfer, M. Trautmann, J. Henk, and P. Bruno, *Phys. Rev. B* **76**, 073310 (2007).